2023

Why are some beaches more conducive to surfing? Bathymetric effects on nearshore waves at Croyde

Bailey, J.

Bailey, J. (2023) 'Why are some beaches more conducive to surfing? Bathymetric effects on nearshore waves at Croyde', The Plymouth Student Scientist, 16(2), pp. 1-26. https://pearl.plymouth.ac.uk/handle/10026.1/21849

The Plymouth Student Scientist
University of Plymouth

*The Plymouth Student Scientist, 2023, **16**, (2), 1-26*

Why are some beaches more conducive to surfing? Bathymetric effects on nearshore waves at Croyde

Jonathan Bailey

Project Advisor: Dr Mark Davidson, School of Biological and Marine Sciences, University of Plymouth, Drake Circus, Plymouth, PL4 8AA

Abstract

Good surfing waves require high peel angles, allowing surfers to ride the face of the wave. However, these waves are not present at every beach, leading to some having better surfing conditions than others. The production of high-quality surfing waves requires preliminary transformations such as refraction, to occur on the nearshore wave field. Mead and Black (2001), previously assessed how various bathymetric combinations, or components, affected the wave field at world-class surfing breaks. More recently, many articles have been published as a result of advancements made in numerical wave modelling, enabling a comprehensive evaluation of the impact these components have on the nearshore wave. While not focused on surfing, such studies as Rijnsdorp et al. (2020) were successful in quantifying the impact of structures like submerged wave farms on nearshore hydrodynamics, using Phase-Resolving numerical models. In this study, we aim to determine the extent bathymetric features affect the nearshore wave field and how this makes some beaches better for surfing than others. Using a phase-resolving dispersive diffraction-refraction model and high-resolution bathymetry, we identify the key wave transformations which occur due to bottom-induced effects and wave-wave interactions, and then further recognise how these effects alter the wave field, causing better surfing waves at Croyde Beach. The reef, located off Croyde Beach, was found to have a large influence in producing 'A-frame' waves during low tide. This was primarily due to wave focusing caused by incident waves that were refracted around the reef. The shape of the reef influenced the location of the focusing focal point, resulting in higher-quality waves at Croyde Beach rather than the closely located, Saunton Sands. This shows offshore morphology has a big effect on the presence and location of these better-quality surfing waves, and efforts to preserve these waves could start with the preservation of these features.

Keywords: Nearshore, Waves, Wave Model, 2D Numerical model, Beach morphology, Coastal dynamics, Surfing.

Introduction

Near-shore Wave Dynamics

Shallow water waves in the nearshore undergo dynamically complex processes, causing wave crests to vary in direction and characteristics. When entering shallow water, physical processes such as Refraction, diffraction, and nonlinear effects of wave-wave interactions transform the wave field characteristics (Afzal & Kumar, 2022). These processes are primarily driven by bathymetry, with complex irregular and steep bottom topography resulting in increased wave transformations, such as wave height along the wave propagation path (Battalio et al, 2005). The transformation of linear deepwater surface waves is a well-understood and documented field, however, there is significantly less research on the effect complex bathymetry has on wave transformation within the nearshore (Chen *et al.*, 2018). The result these processes have on the generation and propagation of high-quality surfing waves is even more limited. As mentioned by Belibassakis *et al.* (2001) this is partially due to the complex nature of the calculations involved with predictions using models.

Refraction

Waves start interacting with the seabed at a depth of less than one-half the wavelength, from which they then experience a change in wavelength and therefore change in wave speed (Wolf, 2008). Irregular changes in speed along the crest cause a change in the wave propagation angle and the waves ‘bend’ towards areas of reduced wave speed (Battalio *et al.*, 2005). Often such as in Joevivek *et al.* (2019), within the nearshore, refraction causes waves to become normal to the shoreline. Waves parallel to a straight uniform contour beach often form later mentioned closeout waves which are undesirable to surfers (Hutt *et al.*, 2001). Furthermore, the refraction of waves often causes converging or diverging wave paths resulting in increased and decreased wave energy respectively.

Diffraction

Diffraction is a phenomenon in which energy is laterally distributed along the length of individual wave crests (Monk *et al*., 2013). This is especially important when waves are forced and focused into areas of higher energy concentrations such as through a harbour entrance or bathymetric vertical forcing. In the presence of no diffraction, unrealistic wave heights would form due to energy not dispersing laterally (Battalio *et al.*, 2005). The energy transfer along wave crests causes waves to disperse and spread out when propagating through passages or past the side of a headland or island.

Surfing waves

Wave peel angle

Desirable surfing waves depend on a wide variety of wave characteristics and the level of the surfer. Unless beginners, surfers prefer waves that ‘peel’ laterally along the wave crest, allowing them to sit in the section between the breaking and unbroken crest called the ‘pocket’, where the highest wave energy is found (Hutt *et al.*, 2001). The angle of this peeling (Peel angle (α)) is defined as the angle between the breaking point of the first initial wave crest and the breaking point of a successive wave crest, as depicted in Figure 1A (Hutt *et al.*, 2001). Peel angle can range from 0° to 90°. Small angles no longer allow surfers to stay on the wave face as the entire crest simultaneously breaks, called a closeout (Figure 1B) (Mendonça

et al., 2012). Larger angles reduce the speed at which the peeling happens, therefore making a less ideal wave for short boarders (surfers using small boards) (Scarfe *et al.*, 2003). The peel angle has been used to categorise the difficulty of waves allowing us to determine if a wave is surfable or not (Hutt *et al.*, 2001).

A-frame waves

Where waves are focused into a peak and breaking is induced, 'A-frame' waves can be produced where the wave crest peels laterally both left and right of the initial breaking point (Figure 1C) (Black & Mead, 2009).

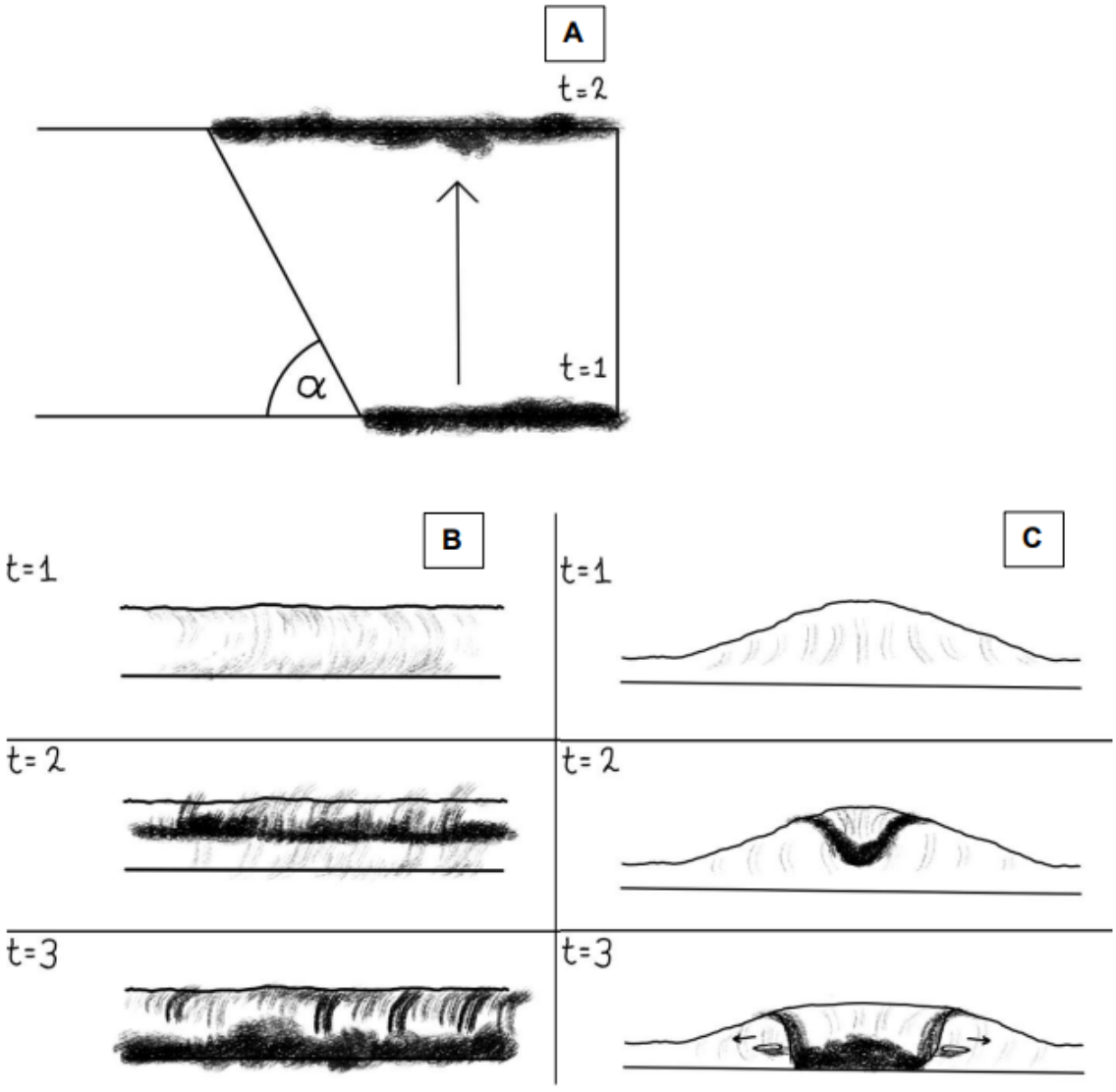

Figure 1: shows A, the process of acquiring peel angle (α). The arrow shows the direction of travel of the breaking wave through an increment of time shown by the initial crest t=1 and the finial t=2. Using two different waves as shown in the figure you can determine the peel angle (α). B shows the transformation, over 3 increments of time, of a breaking close-out wave. Note the crest breaks simultaneously. C shows the transformation of a breaking A-frame wave, over 3-time increments. The two arrows at t=3, show how surfers would be able to surf either left or right from the initial breaking peak. A was an adaption from Hutt *et al.* (2001).

This allows A-frame waves to harbour two surfers at once and allows the choice of surfing either the right wave face or the left face making them favourable. Some of the best-known surfing locations form A-frame waves most notably: Half Moon Bay, California (Mavericks); Praia do Norte, Nazare, Portugal and Pipeline, Oahu Hawaii.

Numerical wave modelling

In recent years numerical wave models have become a vital resource for determining shallow and nearshore wave field characteristics. Two of the most prevalent and early numerical models are The Wave Model (WAM) produced by Hasselmann et al (1988) and Simulating Waves Nearshore (SWAN), developed by Booij et al (1999). WAM was produced to combat the disparity between predicted wave heights of numerous first-generation models at the time (BODC, 2022). However, WAM does not reliably produce results in water depths of less than 30m, primarily due to rudimentary shallow-water equations and restrictions in resolution, leading to an inability to resolve small-scale bathymetric effects as well as triad interaction predictions and depth-induced wave breaking (Booij *et al.*, 1999; Rogers, 2020). Being the main mechanism for nearshore wave dissipation, depth-induced breaking is crucial for resolving nearshore waves (Westhuysen, 2012). This led to the production of SWAN by Booij *et al.* (1999). SWAN is also a 3rd generation wave model; however, it utilises the Eulerian formulation to describe the evolution of two-dimensional waves while accounting for triad and quadruplet wave-wave interactions, refraction, and depth-induced wave breaking, making the model more suited to near-shore environments (Booij *et al.*, 1999).

SWAN does have limitations, most notably the absence of diffraction due to the Eulerian approach. The lack of diffraction means areas with obstacles, such as near vertical walls, suffer from inaccurate predictions seen by Peak (2004), in which discrepancies in wave heights were determined to be a result of neglected diffraction effects, reducing the contributed energy to non-direct swell paths. This effect was also seen with Benedet *et al.* (2007) where a lack of diffraction, introduced wave shadows behind deep dredged channels.

Using the Eulerian approach means SWAN is a Phase-Averaging model. Phase-averaging models don't treat waves individually but as a wave spectrum instead (Rogers, 2020). This results in averaged wave height and propagation pattern outputs. Phase-resolving models can preserve the phase information of individual waves which enables these models to accurately predict constructive and destructive interference patterns arising between the incident, scattered and radiated waves (Rijnsdorp *et al.*, 2020; Zhang *et al.*, 2022). Additionally, phase-resolving models, as opposed to phase-averaging models, can model diffraction, retaining important nearshore dynamics. As shown by Varying et al. (2021), when comparing the nearshore wave heights and placement of focusing, between BOSZ a phase-resolving model and SWAN a phase-averaging model, the lack of diffraction can cause a significant difference in predicted results.

Previous studies

To determine the wave propagation passing rough bathymetry over a large area, Afzal and Kumar (2022) used SWAN with a phase-decoupled refraction-diffraction approximation to counter the normal issue of lack of diffraction seen in phase-averaging models and therefore, produced more accurate wave field predictions over a large area. Peak (2004) also carried out a similar study determining the effects of refraction on the nearshore wave climate due to rough bathymetry. It was

found that the canyon located in the study area had a significant effect on the propagation of the swell waves and caused large variations in wave heights across the canyon. Although the model predictions were concluded to follow observational data, as mentioned above the lack of diffraction implemented in the model often over-predicts wave heights in areas of wave energy focusing. In contrast, Mendonça *et al.* (2012), made use of a phase-resolving, non-linear, multilayer wave propagation model, named COULWAVE and produced by Lynett *et al.* (2004), to determine the beneficial effect and characteristics caused by the refraction of wave rays over an artificial reef. Rijnsdorp *et al.* (2020) also made use of a phase-resolving model to determine the nearshore effect with the presence of a subsurface wave farm. While not based specifically on bathymetry this study highlighted the impact offshore transformation such as converging flow patterns, caused as waves pass into reduced depth, can have on waves at the coast. (Mead & Black, 2001) classified using field studies, the effect certain bathymetric features or components have on swell waves as they pass over. This enables us, through the use of bathymetric data, to categorise certain features and predict the effect these might have on the wave field. However, this study doesn't allow us to analyse the extent to which located features would have on specific locations, therefore further numerical modelling analysis would need to take place.

Croyde Bay

Located in the northwest of Devon, Croyde beach (figure 2) has earned a reputation for the aforementioned 'A-frame' waves. The waves formed at Croyde Beach have led to its classification as a World surfing reserve. World surfing reserves aim to preserve the wave and surfing conditions of the specified beach (Save the Waves Coalition, 2023). To preserve the surfing break, a comprehensive understanding needs to be had of how the waves transform and propagate as they enter the nearshore. Understanding how 'world-class' waves are formed from natural bathymetry and the overall wave climate also helps the production of artificial surfing reefs which are designed to provide good surfing waves, such as that at Cables Reef, Perth. Artificial reefs Increase the number of surfing locations and decrease crowding, often seen at popular wave breaks.

South of Croyde beach is Saunton Sands (figure 2). While being close to Croyde Beach geographically, Saunton has a dissimilar wave characteristic and is suitable for beginners and surfers using longer surfboards(longboarders), which desire greater peel angles (Scarfe *et al.*, 2003). This fuels the question of why two seemingly similar beaches can have vastly differing wave climates.

This study aims to ascertain the degree to which bathymetric factors contribute to the varying wave surfing climates observed at various but related beaches. To achieve this, the effect complex bathymetry has on the nearshore wave field transformation and propagation needs to be analysed. This will be done using a modern numerical wave model, accurate in predicting nearshore propagation paths and wave-wave interactions.

Methodology

Wave data analysis

Real-world data on the conditions found in deep water off Croyde needed to be collected to provide the boundary conditions to the model. Wave data can be collected through various methods, one of which is through wave buoys, as used by the Plymouth Coastal Observatory (PCO). The PCO utilises a Datawell Directional

WaveRider MK III buoy which can measure wave heights to +/-3% and wave direction to +/-1.5°. One of these buoys is located at Bideford Bay, seen in Figure 2. While not ideal deep-water conditions at approximately 11m depth, the Bideford Bay buoy will provide accurate and extensive data on incident waves in the regional area. It should be noted though that this location of the buoy could have a potential effect on the perceived 'normal' conditions offshore at Croyde. The Bideford wave buoy has collected multiple years of data, sampled into 30-minute bins, providing a large dataset to analyse. The dates span from 17th June 2009 to 31st December 2022.

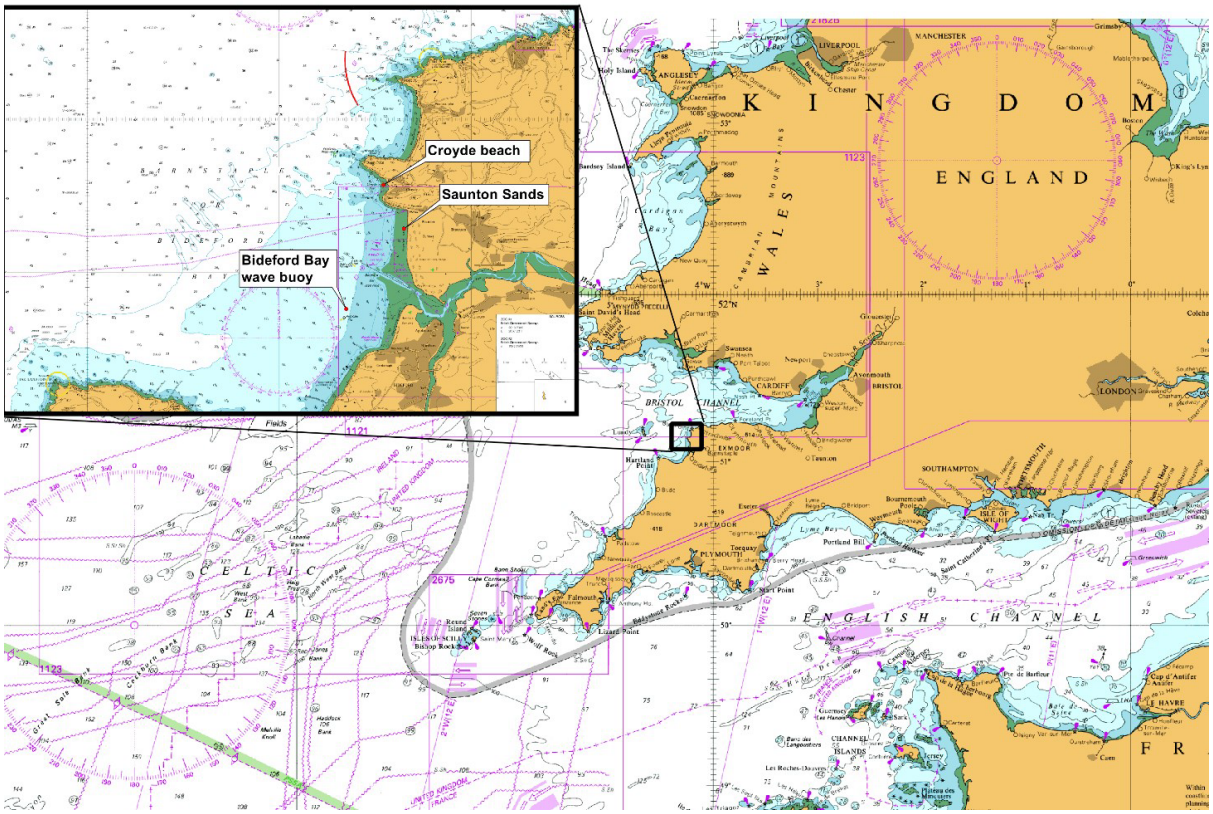

Figure 2: shows the survey location for this study in relation to the United Kingdom. Labelled are the key locations of this study: Croyde Beach, Saunton Sands and Bideford Bay where the wave buoy is located. The map was acquired and adapted from Digimap. Raster Charts [TIFF geospatial data], Scale 1:50000, Tiles: 1164-0, Updated: 18 January 2023, OceanWise, using: EDINA Marine Digimap Service, <https://digimap.edina.ac.uk>, Downloaded: 2023-03-22 15:55:17.703. Marine Themes Vector [FileGeoDatabase geospatial data], Scale 1:25000, Tiles: GB, Updated: 25 August 2022, OceanWise, Using: EDINA Marine Digimap Service, <https://digimap.edina.ac.uk>, Downloaded: 2023-03-22 15:55:17.703

To determine the dominant wave conditions, the wave data first needed to be checked for normal distribution. Through the use of a One-sample Kolmogorov-Smirnov test, Significant wave height (H_s), Time period (T_p) and Incident wave direction(θ) were tested for the null hypothesis that the data came from a standard normal distribution. Where nonnormal distribution was found, the median was used.

Chosen numerical model

For this study, the shallow to intermediate water depth at the location requires a numerical model which not only accurately models key physical phenomena such as refraction, diffraction, and wave-wave interactions, but also has compatibility with high-resolution steeply varying bathymetry. Phase-averaging solutions like the commonly used SWAN model work well in shallow waters however, diffraction is not well-modelled and is most accurate in phase-resolving models (Rogers, 2020). Therefore, in this study, a Phase-Resolving approach would be more suitable. The model used is a Phase-resolving wave model based in a MATLAB environment from Koutitas and Scarlatos (2015), which was then altered by (Davidson, 2021, Pers.com.) to accept bathymetry. The model utilises the formulation below (Equation 1) to determine a horizontal two-dimensional domain for linear, dispersive, long waves, including bed friction and wave breaking.

$$\frac{\partial^2\zeta}{\partial t^2} = \frac{\partial}{\partial x}\left(c_0 c_g \frac{\partial\zeta}{\partial x}\right) + \frac{\partial}{\partial y}\left(c_0 c_g \frac{\partial\zeta}{\partial y}\right) - \left(\sigma^2 - k^2 c_o c_g\right)\zeta - \lambda\frac{\partial\zeta}{\partial t} + N_b\left[\frac{\partial}{\partial t}\left(\frac{\partial^2\zeta}{\partial x^2}\right) + \frac{\partial}{\partial t}\left(\frac{\partial^2\zeta}{\partial y^2}\right)\right] \quad \text{Equation 1}$$

Where ζ is the free surface elevation, c_g is the wave group velocity (ms^{-1}), c_0 is the phase speed (ms^{-1}). σ is the angular frequency where $\sigma = \frac{2\pi}{T}$ and T is wave period(s). K is the wave number where $k = \frac{2\pi}{L}$ and L is the wavelength. λ is a dimensional coefficient (s^{-1}) and N_b is the energy dissipation in the breaking zone due to turbulence and is comparable to the eddy viscosity coefficient.

The model, while providing an accurate prediction of the wave transformation along its propagation, does have limitations. One of these being its classification as a propagation-only model, therefore, the model does not take into consideration any further inputs in wind energy along the fetch, producing and adding no further energy into wind waves in the domain than that produced at the boundary (Battalio *et al.*, 2005). Wave spread is also not computed or included along the boundary, making the model assume and produce Monochromatic wave conditions in a straight line along the boundary (Ris et al, 1999). In reality, incident waves along the boundary would be a mix of secondary and tertiary swell waves propagating at alternative angles and parameters.

From the model, we can extract the wave height root mean squared (H_{rms}), which is then averaged for the length of the simulation. This allows for the assessment of averaged wave heights in the domain, displaying any localised areas of increased or decreased wave H_{rms}. Due to the monochromatic waves being radiated at set time periods from the boundary, aliasing is likely to occur on the H_{rms} averaged outputs.

Bathymetry

The bathymetry input for the model, needed to be at high spatial resolutions to resolve sharply varying features. 2m gridded bathymetry of Croyde Bay and the surrounding area as seen in Figure 3 was provided by Dr Christopher 'Kit' Stokes and was collected using both Light detection and ranging scanners and multibeam

echosounder, ensuring accurate measurements for both the seabed and tidal zones. Due to computational power limitations, the bathymetry was then downscaled to a 20m grid which is still sufficient to depict key bathymetric features such as reefs.

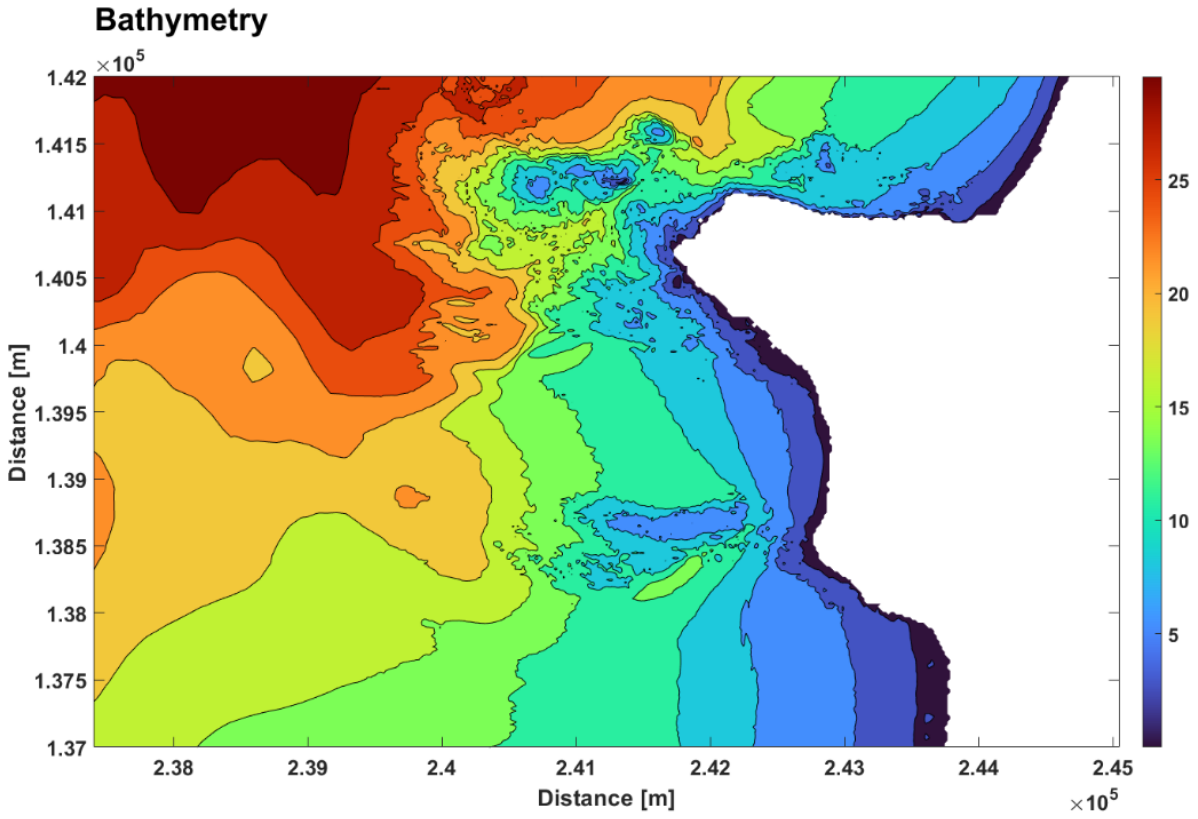

Figure 1: depicts a contour map of the bathymetry data for Croyde Bay and Saunton Sands. The depths are taken to chart datum. The reef located in zone a is a key location in this study. Data provided by Dr Christopher 'Kit' Stokes.

Model stability

The model used utilises an explicit formula meaning, that if instability is present large errors can build up resulting in inaccuracies or a complete crash. To prevent this, when using the 20m bathymetry a suitable timestep needs to be set. The Courant-Friedrichs-Lewy condition (Equation 2) enables us to determine the stability of the model's 2-dimensional domain in its current state.

$$C = \frac{u_x \Delta t}{\Delta x} + \frac{u_y \Delta t}{\Delta y} \qquad \text{Equation 2}$$

Where u (ms^{-1}) is the initial deepwater wave speed at the boundary in either the x or y direction, Δt (s) is the time-step and Δx (m) is the horizontal grid size and Δy (m) is the vertical grid size. If C ≤ 0.5, the model is stable. Using the computed median wave period and 20m grid, a time-step of 1 resulted in a Courant number of 0.2, making the model stable (Table 1)

Table 1: shows the calculation of the 2-dimensional Courant-Friedrichs-Lewy condition.

Wave Speed (Deepwater)			
g (m/s)	**T (s)**	**Pi**	**U_x (m/s)**
9.81	10.50	3.14	4.05

Courant Number (2d)					
U_x (m/s)	**U_y (m/s)**	**t (s)**	**y (m)**	**x (m)**	**C**
4.05	0	1	20	20	0.20

Key: g is the acceleration due to gravity (ms^{-2}). T is the wave time period (seconds). The deep-water equation $\boldsymbol{u} = \sqrt{\frac{gT}{2\pi}}$ is used to calculate the initial deep wave speed. The courant number is calculated from u (ms^{-1}) the deep-water wave velocity, which is represented in the x and y direction of the numerical grid. t(s) is the time step the model is using. y (m) is the grid vertical grid resolution and x (m) is the horizontal resolution.

Tidal data

Tidal level has a big impact on the result and characteristics of wave heights in the nearshore (Lewis *et al.*, 2019). In its initial state, the model takes the bathymetry relative to the chart datum. The computed domain water level would be defaulted to the minimum tidal level resulting in the largest degree of bottom-interaction effects. As the tides change, waves experience differing levels of bottom-induced effects therefore, tide and water level adjustments needed to be implemented into the model. This was done by decreasing the depth of the initial bathymetry at the start of the model, artificially increasing the water height, and resulting in a higher tidal level. Tidal data was collected using a PCO tidal gauge located at Port Isaac. This tidal gauge samples every 10 minutes. The maximum tidal level was taken as the median of the maximum monthly tidal heights (Figure 4). This median value was measured as 8.1m, which aligns with data shown in the UK Renewables atlas (Accessed: 10/03/2023) for the tidal range.

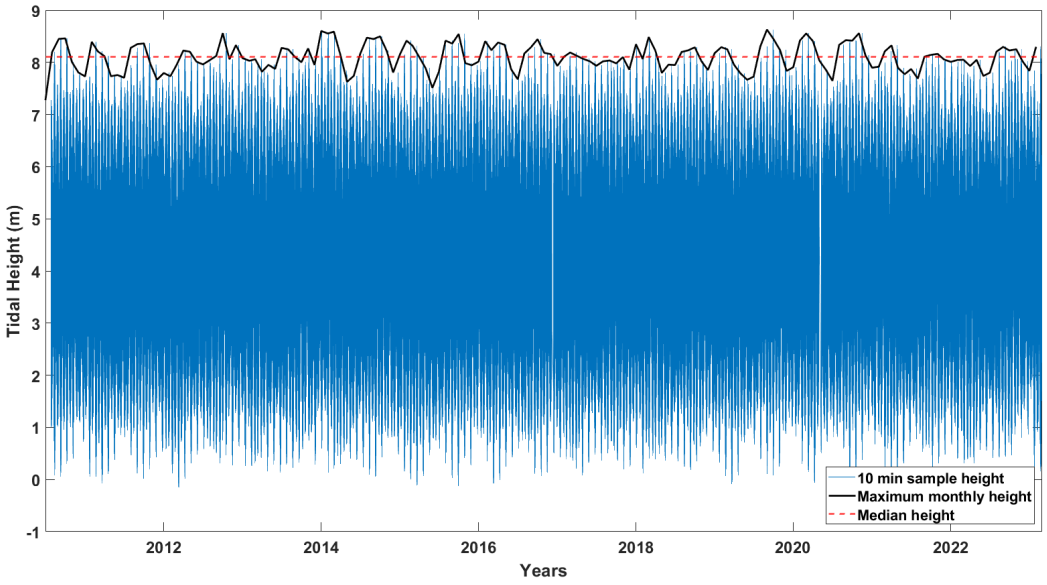

Figure 2: is the tidal height data relative to chart datum, collected from the PCO (Plymouth Coastal Observatory) tidal gauge, located at Port Isacc. The Black line represents the maximum monthly tidal height of the 10-minute sampled heights (blue). The median shown as a dashed line is then taken from this maximum tidal height. The median tidal height for the maximums is 8.1m.

Sensitivity analysis

Sensitivity analysis was carried out to determine the effect and sensitivity of the model to changes in the eddy coefficient (ec), reflection coefficient (rc), and breaker index (γ_b). Due to the nature and limitations of this research, real-world data collection of wave characteristics at the Croyde Bay area was not viable. This meant outputs of the models were not able to be compared with a real-world scenario. Consequently, for the sensitivity analysis, the values of ec, rc and γ_b were individually altered for an extreme upper and lower bound and the extent of the effect was evaluated. Values of rc were varied with a minimum ec to allow waves to reflect from the beach and not dissipate before being able to reflect. A transect of the nearshore and breaking zone was taken for each of the parameter adjustments for comparison (Figure 5). A one-sample Kolmogorov-Smirnov test was performed on the transect to determine normality, with a $p<0.05$ the null hypothesis of normality is rejected. Where, $p<0.05$, a Wilcoxon rank sum test is then used to determine the significance between the upper and lower bound transects. If $p<0.05$ for the rank sum test was found, there is significance between the two transect wave H_{rms} therefore, careful consideration of the value being used for said parameter would have to be taken, so as not to cause inaccurate or unrealistic results.

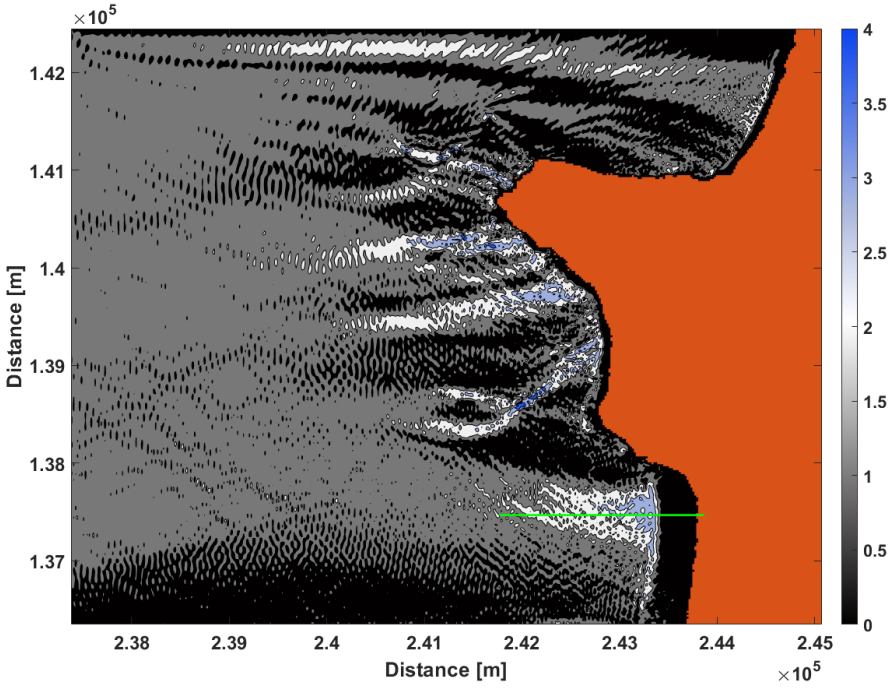

Figure 3: shows the location of the transect used for the sensitivity analysis. The transect is shown as a green line and intersects the breaking zone of Saunton Sands.

Non-normal distribution was found for all the transects therefore, the Wilcoxon rank sum test was performed for each parameter. Figure 6A shows the difference between an upper rc of 1 and a lower of 0.1. The rank sum test returned a value of high similarity between the two conditions of $p = 0.954$. This means the choice of rc should not significantly vary the output of the model. It is common however, for beaches to be increasingly reflective towards the high-water mark, therefore rc was also analysed at the maximum tidal height (Elgar *et al.*, 1994). At high water, the rc p value was seen to decrease to $p=0.392$ (Figure 6B) as a result of an increased reflection effect. This p-value verifies that there is still no significant difference between the upper and lower rc values. In Figure 6C, the difference in an upper ec of

1 and a lower ec of 0.1 is shown. Again, similarity between the data was found with p = 0.700 however, there is more difference seen than rc, with a greater difference most notably in the breaking zone where dissipation due to turbulence would be taking place. In the final figure 6D, the γ_b bounds are compared with an upper of 1.4 and a lower of 0.4. The model is the most sensitive to this parameter with a p-value of 0.006 meaning there is a significant difference between the upper and lower bounds therefore, the value chosen could have a significant effect on the model results. In the models operation, a γ_b of 0.78 will be set, as solitary wave theory permits this as a good first-order approximation (Masselink, 2019).

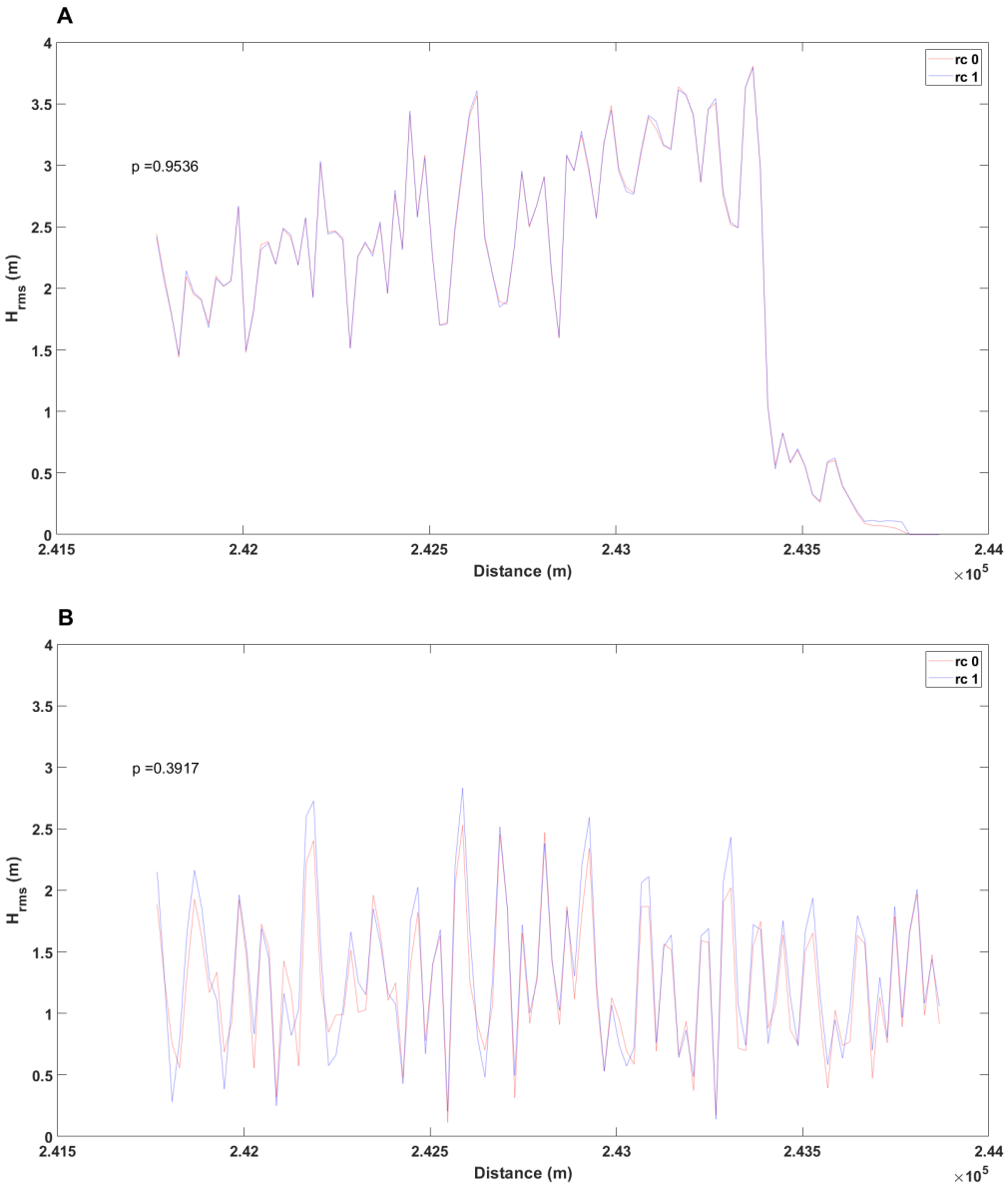

Figure 4 (A and B): shows the Hrms (m) for the length of the breaking zone transect. A shows Hrms (m) for the reflection coefficient (rc) values of 0 (red) and 1 (blue). These transects resulted in p=0.9536. B shows the Hrms (m) for the rc values during high tide of 0 (red) and 1 (blue). The p-value for these was 0.3917.

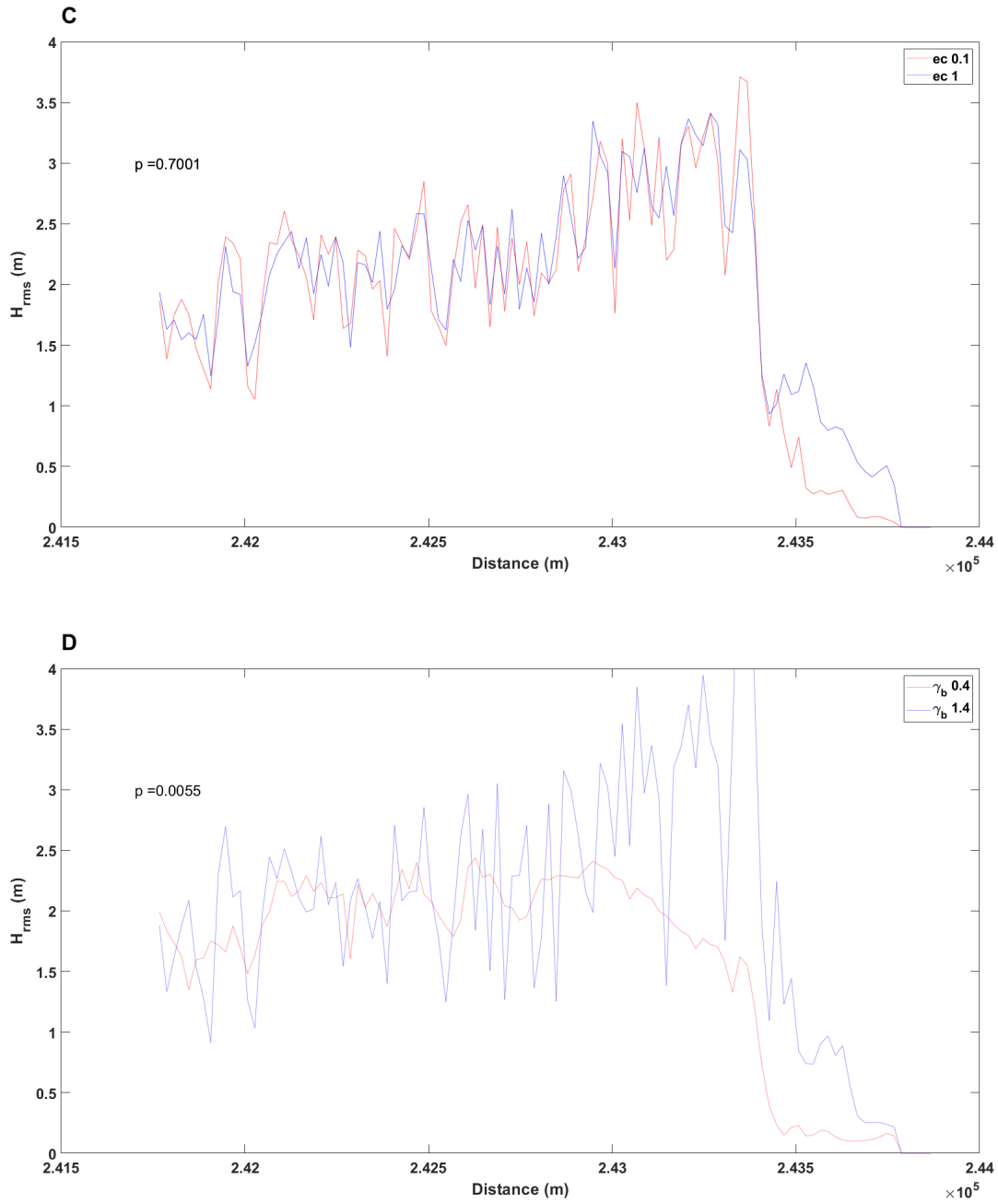

Figure 5 (C and D): C shows H_{rms} (m) for the eddy coefficient (ec) values of 0 (red) and 1 (blue). For this parameter p=0.7001. D shows H_{rms} (m) for the breaker index (γ_b) values of 0.4 (red) and 1.4 (blue). P=0.0055 making the transects significantly different. This is seen in the figure as on the lower γ_b bound of 0.4 the waves dissipate earlier at 2.5m than the upper bound.

Results

Wave data analysis

The test is shown to reject the null hypothesis for each wave parameter, confirming the data as not being normally distributed. Therefore, median values for T_p, H_s and θ_D are found and used in the model as the dominant wave conditions at Croyde Bay (Figure 7). The median value for H_s was identified as 0.96m and 10.50s for the T_p. For the θ, the median was 281° from the north. This means the input value to the western boundary is taken as 11°.

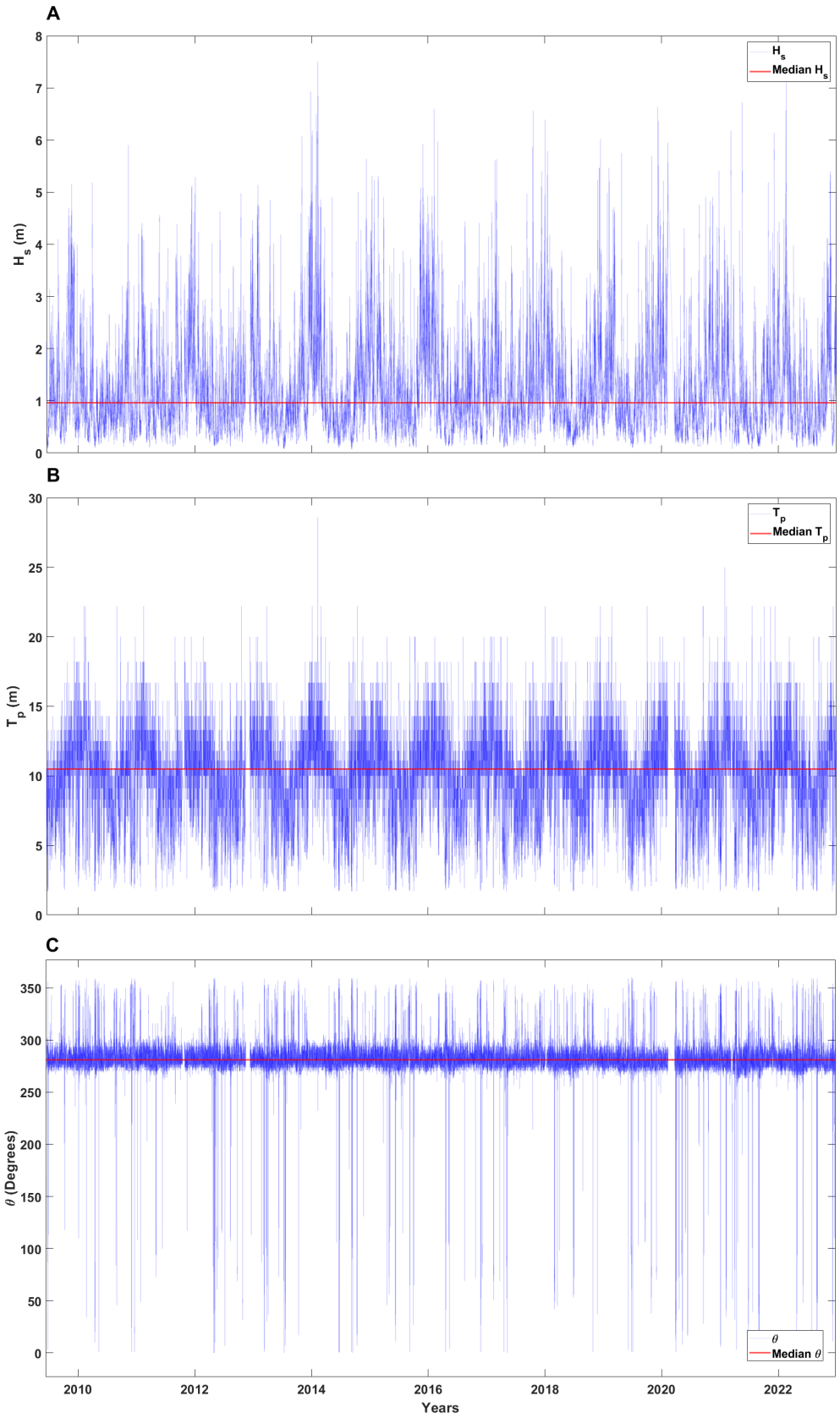

Figure 6: shows the wave analysis carried out on the data from a PCO (Plymouth Coastal Observatory) wave buoy, located at Bideford Bay. A shows the raw data (blue) for the significant wave height (H_s (m)) over multiple years. The red line depicts the median value for H_s at 0.96m. B shows the raw data of wave time period (T_p (s)) (blue) from 2010 to 2022. The red line depicts the median T_p of 10.5s. C displays the raw incident wave angle (θ (°)) data from north. The red line shows the median θ of 281°.

Wave propagation

Using the median wave conditions, the effects of the bathymetry on the wave transformation and propagation are identified. The first output seen below (Figure 8A) shows the propagation of median condition waves, at the lowest tide in relation to the chart datum. The first key location is the refracting waves at position (a), which are located over a shallow reef, labelled 'a' in the bathymetry (Figure 3). The refracting wave bends northwards, towards and onto Croyde beach, while superimposing with waves refracting southerly. The refracted waves then continue onto the middle of Croyde Beach leaving a shadowed zone leeward of the initial refraction. Contrary to the northward path, there is a large general trend of a southerly refraction in the wave field, curving the wave crests right making an eastern propagation path therefore, making the waves initially more parallel to the coast. Furthermore, while the waves are refracted into the middle of Croyde at an angle, at the northern end of both Croyde Beach and Saunton Sands, the waves are seen to continue to propagate on a more direct path into the beach. At the southernmost boundary, it should be noted that there is an area of 'shadowed' waves. This is due to the model only producing waves at the western boundary and with the swell propagating at 11°, the shadowed area is formed.

Changing the tidal height to 8.1m relative to the chart datum gives the simulation of the highest tidal level (Figure 8B). The previous refraction occurring at point (a) is less pronounced with less propagation path change. The limited refraction that is still present is located over the main shallow portion of the reef, which refracts the waves to the left before they are refracted back to normal by the beach slope. There is still the presence of a general trend in refraction southwards however, this is to a lesser degree resulting in the previously mentioned shadow, leeward of the reef at low tide, being less pronounced and waves then propagate into the northernmost point of Saunton Sands.

Root-mean-square wave height

In Figure 9A, point (a) over the reef, there is increased wave H_{rms} of up to 3.2m at the southern side of the reef which then bends shoreward in a diagonal band. At the northern side of the reef, there is again a wave H_{rms} increase from 1.2m to 3.7m as the waves propagate over the shallower water of ~5m depth. This then intersects the southerly side increase, at the leeward edge of the reef where the waves peak up to 4.9m. This band then shortly decreases before culminating at Croyde beach where there is a further and final increase of H_{rms} up to 3.8m. At Saunton sands, there is a relatively gradual H_{rms} increase during low tide, from 1.6m in the nearshore to 3.7m at the breaking zone as the waves propagate into the beach over the gentle slope (zone b). During high tide (Figure 9B), the northern area of the reef (point c) experiences an overall reduced wave H_{rms} reaching a maximum of 3.1m directly over the shallowest part of the reef. This increase then continues to Croyde beach albeit at 2.7m maximum unlike that seen at low tide. The southern side of the reef experiences a similar change in that the wave H_{rms} is much lower at 2.5m compared to that seen during low tidal heights. Saunton sands also experiences overall reduced H_{rms} for high tide, coming to a maximum of 3m at the northern area of the beach, decreasing further south to 2m.

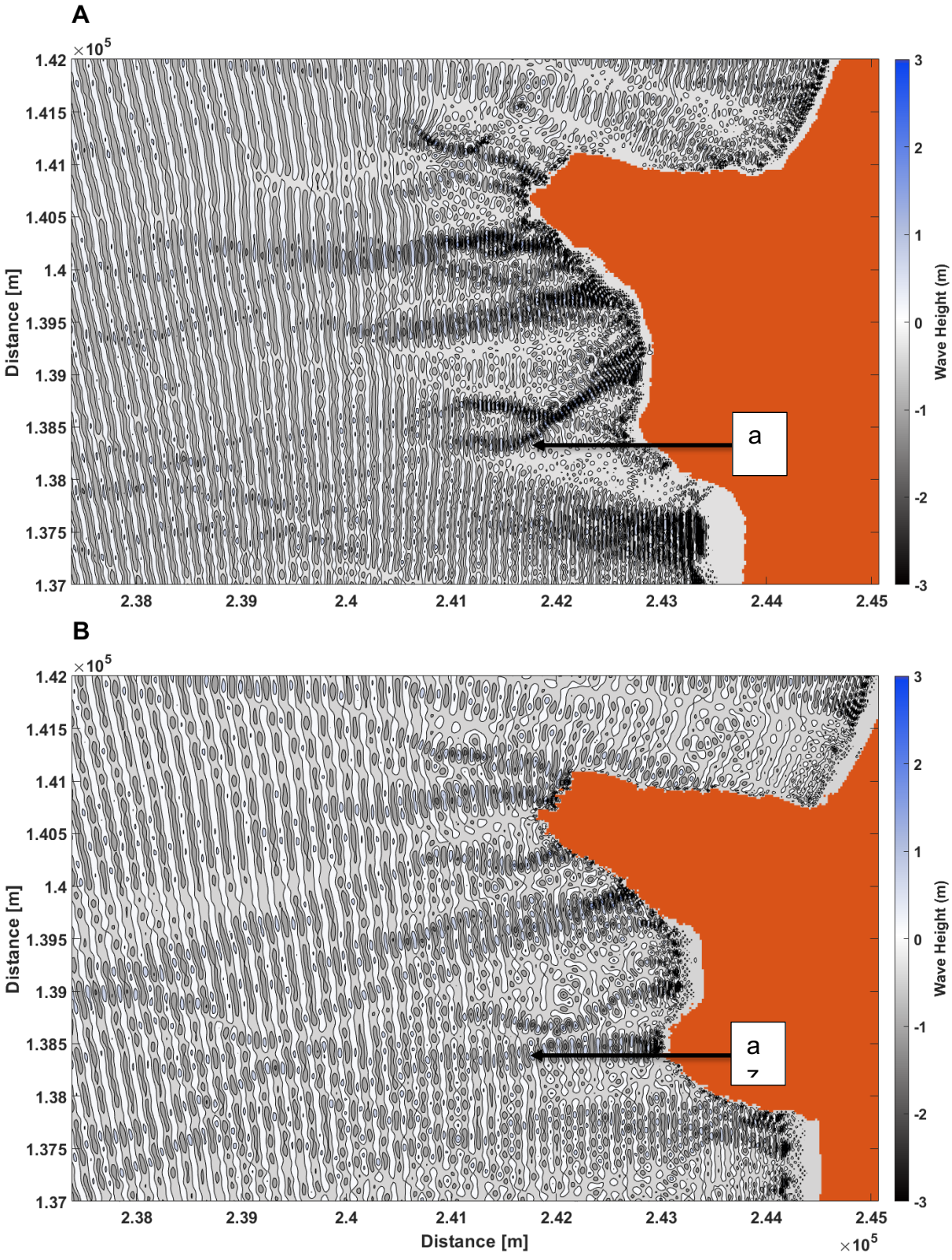

Figure 7: shows the low (A) and high (B) tide wave propagation in the survey area. Point a depicts a key refracting effect which is seen clearly in A but is much less pronounced in B. Where there are darker areas, these show a larger wave height change on the domain surface.

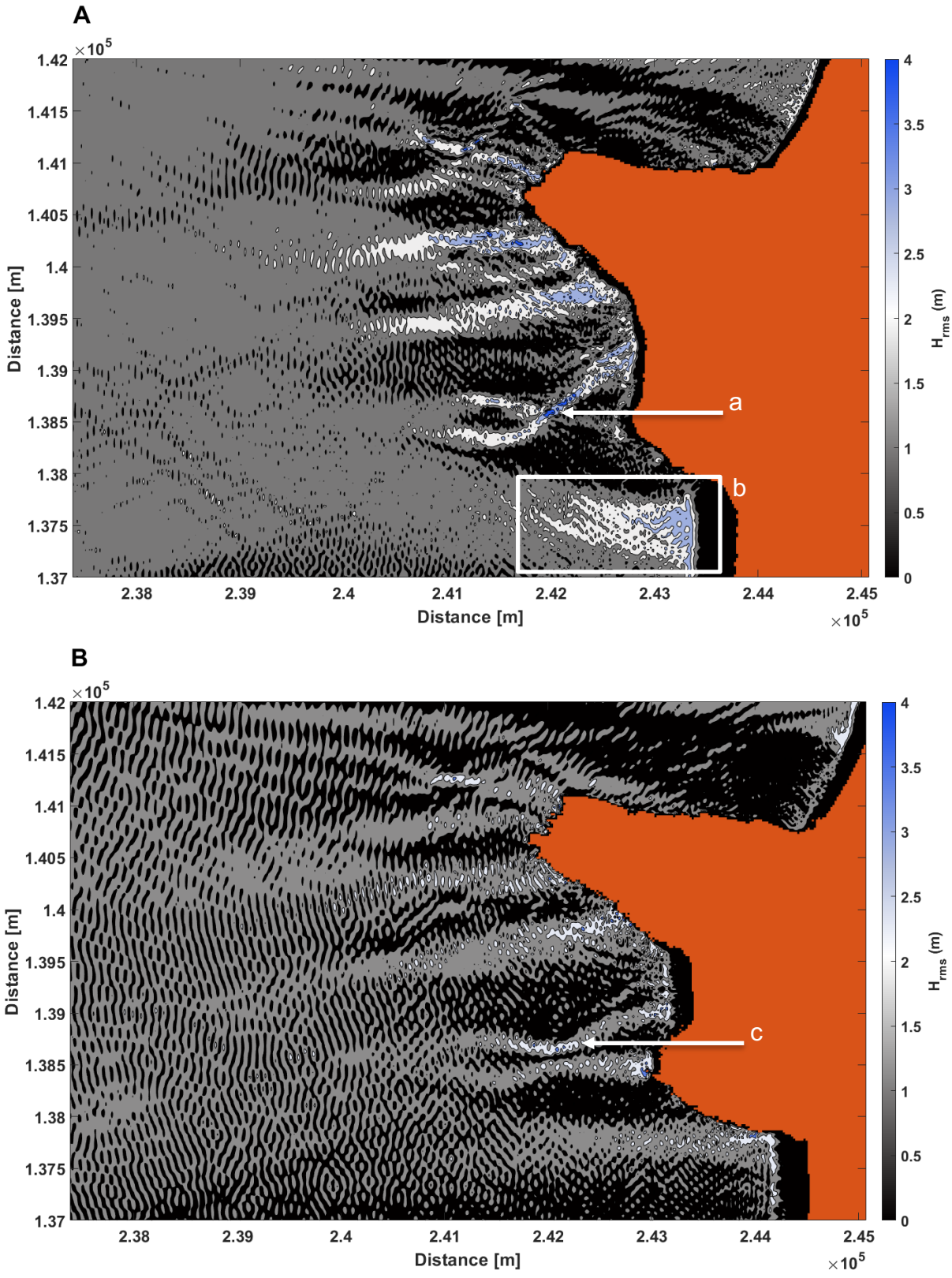

Figure 8: shows a contour of low (A) and High (B) H_{rms} over the domain. Where blue contours are seen this represents higher H_{rms} while white represents mid values and black represents low. Point a shows a peak in H_{rms} on the leeward edge of a reef. Zone b shows a gradual increase in H_{rms} as the waves propagate into Saunton Sands. Point c depicts an area of slightly elevated H_{rms} at the northern side of the reef.

Three-dimensional wave surface

Figure 10 highlights the previously mentioned refraction seen in Figure 8, as a three-dimensional wave surface over the bathymetry. During low tide (Figure 10A), the waves on the southern side of the reef are refracted ~45° northward. This refraction follows a similar angle to a trench, seen on the south side of the reef in the bathymetry. The northerly refracted swell then experiences increased wave heights as it is intercepted by the southerly refracted swell from the northern side of the reef. This increased wave height swell then continues at the same angle towards Croyde Beach in a peaked formation. In contrast, during high tide (Figure 10B), no major refraction is seen to take place over the trench on the south side of the reef, with waves passing over and maintaining a similar propagation path. To the north of the reef, over the shallowest part, the waves are seen to propagate slightly southerly.

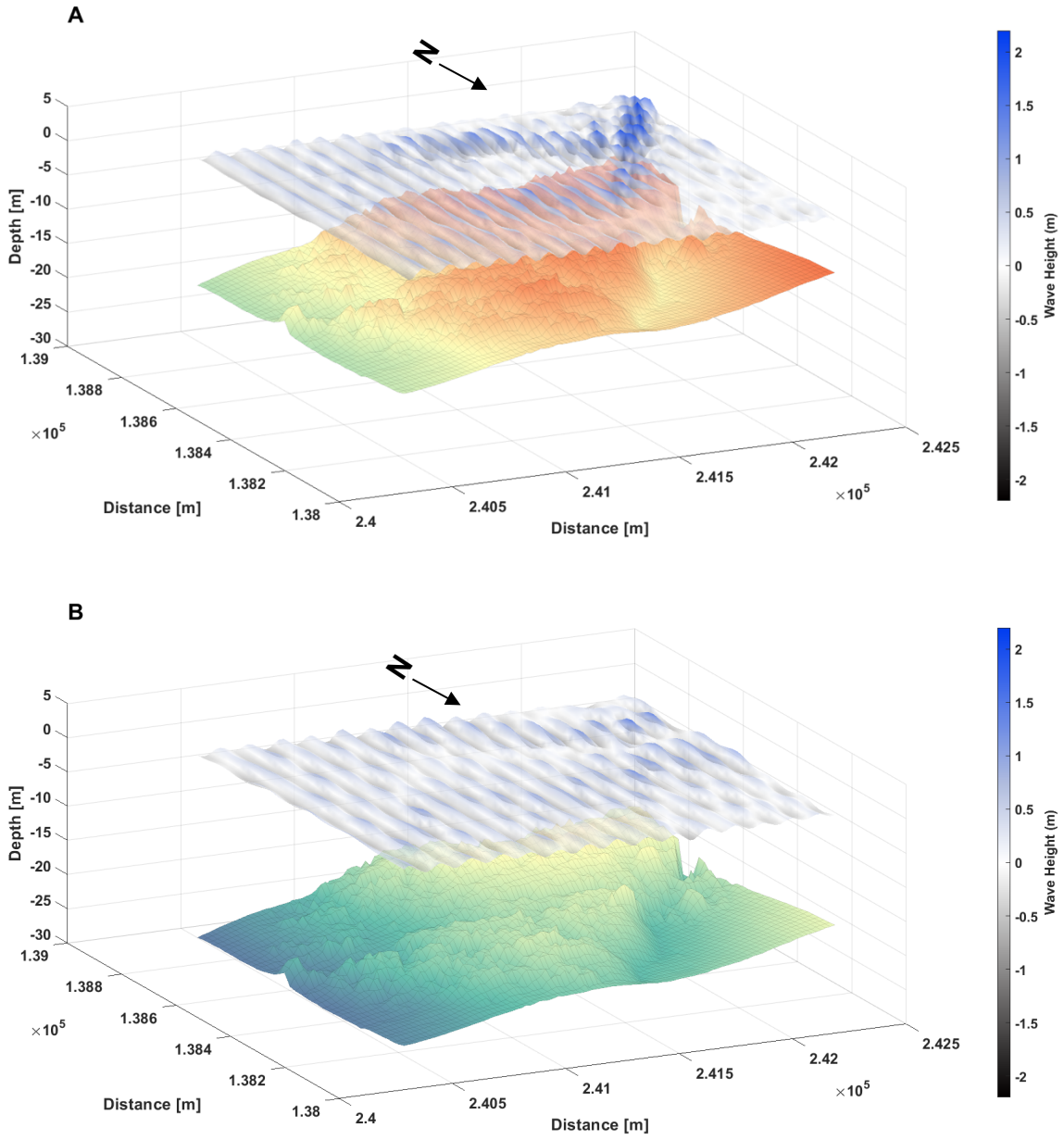

Figure 9: gives the wave surface of the model over the reef during both low (A) and high (B) tide. North is shown as a black arrow and labelled N. Where the waves are shown as dark blue these are the highest wave heights. The depth of the bathymetry is shown on the y-axis.

Nearshore transects

Figure 11A shows the standard deviations of H_{rms}, taken at 0.1m tidal level intervals along a longshore transect at Croyde Beach (Figure 11C).

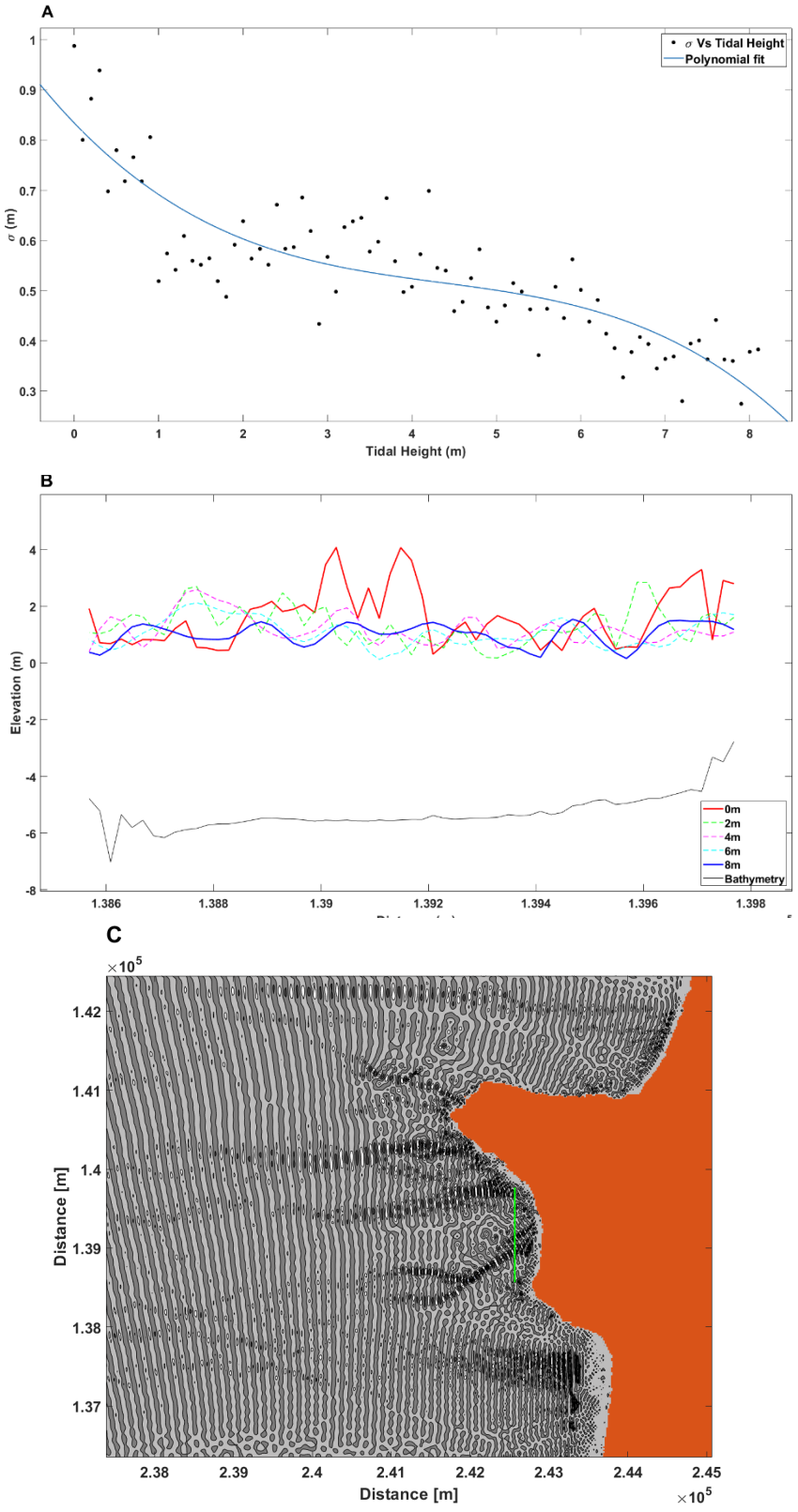

Figure 10 shows the results from the nearshore transect analysis. A shows the standard deviation of H_{rms} (m) against the tidal height (m). The blue line depicts the polynomial fit line using the 3rd order. There is an overall decreasing trend in H_{rms} with increasing tidal heights. B shows the H_{rms} (m) along the length of the transect at 2m tidal height intervals. The two

bound, lower (0m, red) and upper (8m, blue) are highlighted as solid lines to allow for comparison, while the other intervals are shown as dashed lines. The bathymetry is shown as a black line beneath, and its elevation relates to low water (0m).

This makes it possible to evaluate the variation in nearshore wave heights at Croyde Beach throughout an 8.1m tidal cycle. The general decreasing standard deviation with increasing tidal height trend, shown using a polynomial fit, suggests as the tide gets higher the variability in H_{rms} decreases along the longshore transect. The tidal height of 0m has the highest degree of variability at just under 1m of variation from the mean, while the lowest standard deviation is 0.28m at 7.9m tidal height. Figure 11B shows the transect long wave H_{rms} in 2m tidal height intervals with the bathymetry profile below. There are clear peaks in wave H_{rms} up to 4m at 0m tide between $1.390x10^5$m and $1.392x10^5$m on the smooth portion of the bathymetry suggesting, a driving offshore factor. This variability is not seen on the higher tide at 8m with the H_{rms} being less variable and smoother, peaking at 2m.

Discussion

Wave focusing

The south side of the reef located off Croyde Beach (Figure 3), is seen to cause high levels of northward refraction during lower tides. By contrast, the northern side of the reef is depicted refracting waves southerly. These opposing swell propagations cause wave orthogonals to converge and superimpose with each other, concentrating wave energy and therefore, forming a localised area of elevated wave height (Speranski & Calliari, 2001). Figure 12 demonstrates the refraction and subsequent converging of these wave paths, over the reef at Croyde. Known as wave focusing, this phenomenon has been successfully modelled in the past through the use of submerged shoals with circular contours, which demonstrated the refraction of wave paths over the bathymetry, converging into a focal point and causing increased wave height (Ito & Tanimoto, 1972). At Croyde Bay as evidenced by figure 9A there are key focal points, leeward of the reef (position a), where the H_{rms} is also seen to be elevated.

The positioning of the focal point in wave focusing has also been investigated by Mandlier and Kench (2012), who demonstrated that the reef shape is a key deterministic factor. Furthermore, the positioning and manipulation of wave focusing focal points through the use of predetermined artificial bathymetry, has been an idea proposed and tested for increasing the degree of energy capture in wave power generation. Durai Eswaran *et al.* (2020) used similar circular plates as Ito and Tanimoto (1972), to increase the wave height, improving the efficiency of wave energy devices. The reef at Croyde, depicted in Figure 13, has a trench that appears to be the lead driving factor for the level of refraction at the south side of the reef, with the swell appearing to refract and follow the contour north. The same degree of refraction is not seen on the north side of the reef however, resulting in the focusing point being more northerly, propagating waves towards Croyde beach.

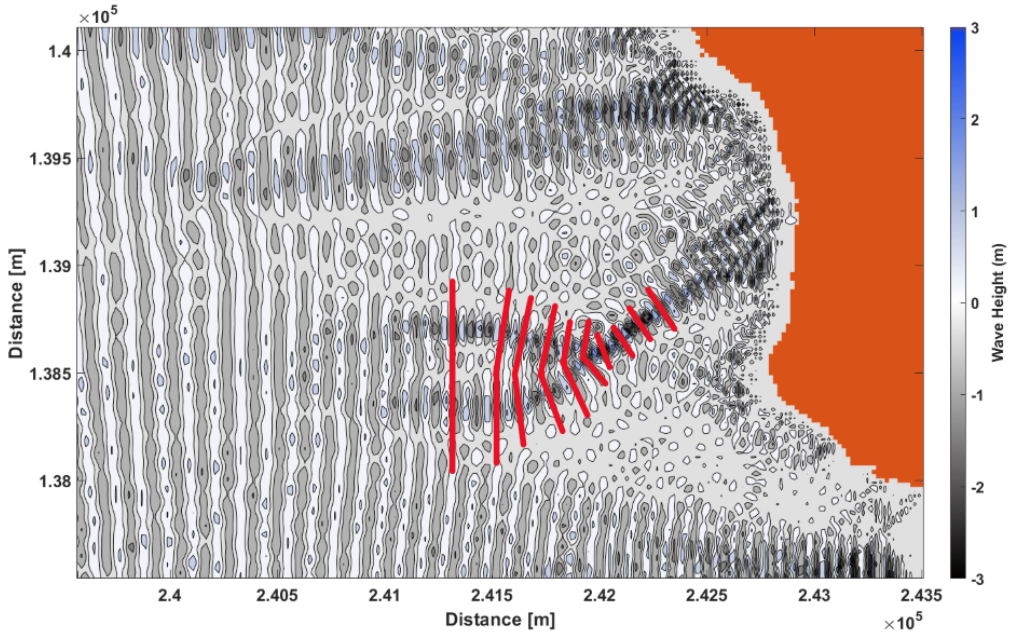

Figure 11: shows how the wave crests, converge into a focal point before propagating into Croyde beach. The red lines represent the wave crest contours and show as the waves pass over the reef and refract the crests converge.

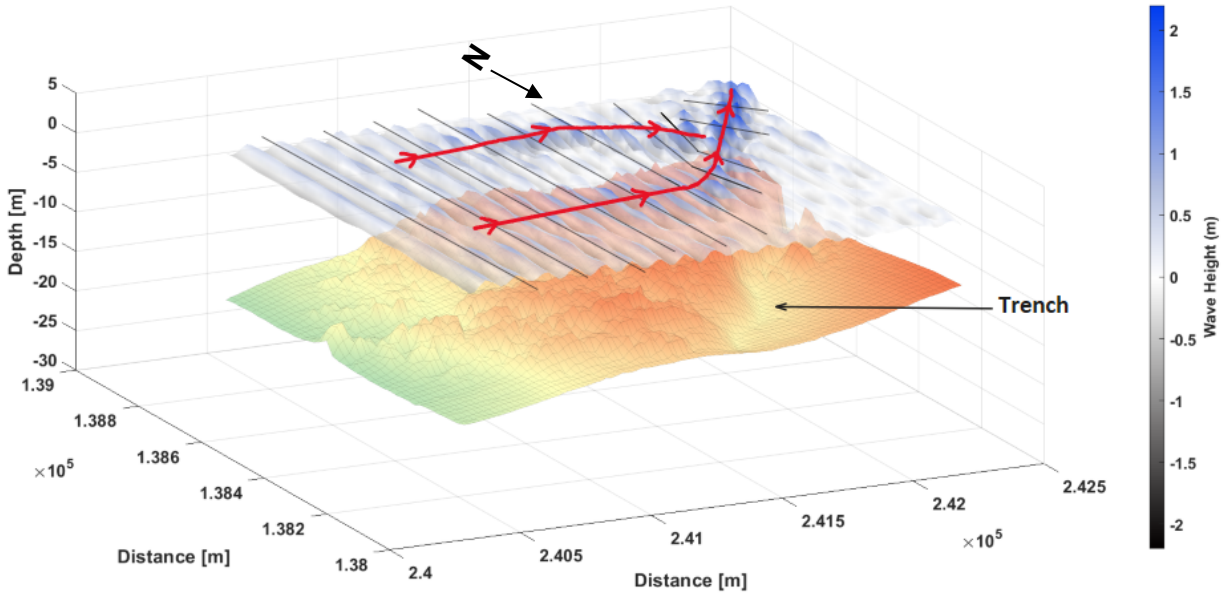

Figure 12: is an annotated figure showing the wave surface over the reef during low tide. The black lines represent the wave crests and are seen to converge. The two red lines represent the wave orthogonals, which converge to a focal point, before continuing towards Croyde Beach. The trench which appears to be driving the northerly (N) refraction is labelled.

Wave focusing is a key component in the formation of A-frame waves. West (2002) highlighted its viability as a concept for new artificial reefs in which A-frame waves can be produced on beaches where closeout waves may have otherwise been. This reef design has been modelled successfully by Mendonça *et al.* (2012) while Black and Mead (2009) on the other hand, conducted scale model testing using a wave-focusing reef on which A-frame waves were successfully produced. During low tide,

Croyde Beach has become synonymous with A-frame waves in the surfing community. The refraction patterns in Figures 8A and 10A support the suggestion that the reef causes natural wave-focusing which then drives the A-frame waves into Croyde beach. Using the classification created by Mead and Black (2001) the reef at Croyde most closely resembles a 'focus' reef component, which is seen producing many other well-known surfing waves such as Pipeline, Hawaii. Furthermore, focus reef components are also said to make taking off (where a surfer catches a wave and initially stands up) easier, allowing bigger waves in height to be surfed thus, making the waves at Croyde potentially better than beaches with harder take-offs (Mead & Black, 2001).

Effect of water level on refraction

At higher tides, the level of refraction is greatly reduced over the reef with the swell propagating on a more uniform path relative to the larger general refraction south (Figure 8B). Costa *et al.* (2019) found a similar result, where an increase in sea level produced a reduction in wave refraction and therefore, a more direct wave propagation over the reef. As the water level increases, the effect of the reef component on the wave propagation also changes, this causes many surfing breaks to have different wave characteristics depending on the water level (Scarfe *et al.*, 2009). This effect was also seen by Black and Mead (2009) who found the results of the artificial wave-focusing reef, producing A-frame waves, were best at low tide. In Figure 9B we are shown the effect reduced focusing has on the wave height. With reduced wave peaking and rms wave height, from 4.9m at low tide to 2.7m at high, A-frame waves are less likely to occur. It should also be noted, that in areas with low tidal ranges, little change in wave transformation processes occurs and thus wave characteristics would stay the same or relatively similar throughout the tidal cycle. Croyde Bay, having an 8+m tidal range, would experience larger changes in wave characteristics and this is reflected in the model (Figure 10).

Wave variability in the nearshore

Figure 11A depicts the relation of wave variability along the nearshore transect against the tidal level. The higher low tide variability is something also seen by Harris *et al.* (2018), in which the lowest tidal height at a reef flat, experienced the highest degree of variation in wave height to water depth ratios. With greater depths the influence of bottom- interactions is decreased, causing bottom-induced effects such as refraction to be reduced, as seen above and in figures 8B and 10B, where the degree of refraction is greatly reduced with increased depth. Most surfing beaches feature preliminary wave transformation by prominent bathymetric morphological features therefore, during higher tides with less bottom-induced transformations, you'd expect a differing or lower surfing quality wave climate (Scarfe *et al.*, 2003). The lower variability and decreased depth-induced transformations seen during high tide point towards a more uniform wave field. Laterally uniform wave crests, propagating normal to a planar beach with parallel contours, have the effect of producing more closeout waves (Figure 1B), with the crest breaking simultaneously at a peel angle of 0 therefore, making it impossible to surf on the wave face (Hutt *et al.*, 2001; Scarfe *et al.*, 2003). This is not a problem for beginner surfers who ride the broken, white-water, sections of waves however, it is not challenging for intermediate or advanced surfers who would rather prefer to surf the wave face, making higher tides often unfavourable (Hutt *et al.*, 2001).

The increased variability at Croyde during lower tides, suggests that the reef could be a big driving factor in the characteristics of the nearshore waves. The large peaks

in the mid-section of the transect in Figure 11B, could show that the waves during low tide are formed into A-frames. The crest would start to break at the middle of the peak therefore forming an A-frame wave and allowing surfers to either surf left or right from the breaking crest. It could be argued that the nearshore bathymetry would have a large influence on the wave variability at the transect. However, as seen in figure 11B the bathymetry along the mid transect is mostly smooth. When at the lowest water level, there are peaks over this section which suggests that the wave transformation is happening further offshore, such as at the reef, and not due to depth-induced forcing locally.

Effect of increased wave height at Saunton Sands

With less water depth, the refraction at the reef is seen to cause a zone of decreased wave H_{rms} or 'shadow', on the leeward side. As the wave path rays propagate northerly and converge on the leeward side of the reef, the southern side instead experiences diverging wave paths. Diverging wave orthoganals cause the opposite effect of wave focusing and as such wave energy is dispersed, decreasing wave heights (Masselink, 2019). The northernmost point of Saunton therefore, has reduced wave heights. In contrast however, during higher water where the general southerly refraction and the northerly refraction from the reef are less present, swell more freely propagates into this northern area of Saunton Sands. This results in high water experiencing increased H_{rms} at the northern end of the beach compared to more southerly (Figure 9B). This is something noted in numerous surf guide websites which suggest the best waves break on the right or northern end of the Saunton sands near the rocky coast (Surfline; Yates). The H_{rms} gradient would likely produce slow pealing waves, due to the non-uniformity of the wave crest height, causing different sections to break at different depths. Low peeling angles would produce better waves for longboarders and beginners which is in complete contrast to the higher peeling angle seen at Croyde Beach (Hutt *et al.*, 2001).

The decreasing gradient in wave H_{rms} at high tide could, however, be a result of the southern boundary condition. As mentioned before, the boundary does not produce incident waves therefore, the waves radiating at an 11° angle from the left boundary of the domain, form a shadow on the southern boundary. In practice, this would not be a shadow with further waves propagating from where the boundary is located. To fully assess the propagation onto Saunton sands, the bathymetry dataset would need to extend further south.

During low tide, where more southerly refraction is present, more waves propagate into Saunton sands. As Saunton Sands is a gently sloping planar beach with uniform contour lines (seen in Figure 3), waves become normal to the beach and increased H_{rms} is observed along the entire surf zone when compared to high water (Joevivek *et al.*, 2019). While the waves can propagate into the beach more freely, the decreasing H_{rms} gradient, seen at high tide, is still present (Figure 9A). This suggests that at high tide with an extended southern boundary allowing more waves to propagate into Saunton Sands, we would likely see a similar increase along the whole beach while still retaining the same gradient, only starting further north near the rocky coast. The similar wave climates at both high and low tide would, suggest the reef has little effect on the surfing wave characteristics at Saunton Sand during median wave incident angles and therefore, would not induce a production of higher quality waves, such as that seen at Croyde Beach.

Conclusion

This paper aimed to determine the extent to which complex offshore bathymetry affected the variability of wave characteristics, and then further answer why some beaches are better for surfing than others. The reef offshore from Croyde (Figure 3), was seen to cause significant refraction, focusing waves during low tide. The focusing caused waves to peak on the lee side of a reef before continuing towards the beach. These peaks form A-frame waves as the crest starts to break. A-frame waves are commonly seen during low tide at Croyde Beach, which granted the area World Surfing Reserve status. This wave focusing however, does not benefit Saunton sands to the south of Croyde due to the reef shape and trench on the southern side, driving the focal point north. Instead, Saunton experiences more direct swell incident waves.

The variability of the nearshore wave crests (Figure 11A) highlighted the importance of the wave focusing by the reef, for creating good surfing waves at Croyde. With reduced bottom influences during high tide and therefore, reduced wave transformations, the wave H_{rms} variation is seen to be reduced. This results in a more uniform wave crest which, increases the probability of closeouts and lower-quality surfing conditions. On the other hand, the variability seen at low tide is higher, with larger peaks being shown mid-transect (Figure 11B) suggested the presence of A-frame waves or waves with lower peel angles, better for more advanced surfing. This means, that without the existence of the reef, Croyde Beach would have lower-quality waves throughout the tidal cycle.

While Croyde Beach benefits from the presence and shape of the offshore reef, producing high-quality surfing waves at low tide, Saunton Sands just south of Croyde, does not, and has a similar wave climate of more direct propagation and uniform wave crest, causing lower quality waves during both low and high tides. The vastly contrasting nearshore wave characteristics between the two beaches, show the influence offshore morphological features, such as reefs, and their spatial structure have on producing and altering the propagation of high-quality surfing waves. Thus, making specific beaches more conducive to surfing than others, even when located in the same regional location. For this reason, organisations, that aim to preserve high-quality surfing waves, should utilise numerical wave modelling, such as done in this study, to determine the effect offshore topography has on the generation of these waves, and therefore allowing for efficient resource management and preservation of key surf break producing bathymetry.

Acknowledgements

Thank you to my advisor Dr Mark Davidson for his exhaustive expertise and help throughout this paper. Thank you also to Dr Christopher ‘Kit’ Stokes for providing the bathymetric scan of the Croyde Bay area. Finally, thank you to my family and Yana Skvortsova for their continued help and support.

References

Afzal, M. S. & Kumar, L. (2022) 'Propagation of waves over a rugged topography'. *Journal of Ocean Engineering and Science*, 7 (1), pp. 14-28.

Battalio, B., Chandrasekera, C., Divoky, D., Hatheway, D., Hull, T., O'Reilly., B., Seymour, D. & Srinivas, R. (2005) 'Wave Transformations'.

Belibassakis, K. A., Athanassoulis, G. A. & Gerostathis, T. P. (2001) 'A coupled-mode model for the refraction–diffraction of linear waves over steep three-dimensional bathymetry'. *Applied Ocean Research*, 23 (6), pp. 319-336.

Benedet, L., Stive, M., Hartog, W., Walstra, D.-J. & van Koningsveld, M. (2007) 'Effects of wave diffraction and initial bathymetric conditions on beach fill volume change predictions'.

Black, K. & Mead, S. (2009) 'Design of Surfing Reefs'. *REEF JOURNAL*, 1

BODC (2022) 'Wave Modelling WAM'. (Accessed: 2022).

Booij, N., Ris, R. C. & Holthuijsen, L. H. (1999) 'A third-generation wave model for coastal regions: 1. Model description and validation'. *Journal of Geophysical Research: Oceans*, 104 (C4), pp. 7649-7666.

Chen, J.-L., Ralston, D. K., Geyer, W. R., Sommerfield, C. K. & Chant, R. J. (2018) 'Wave Generation, Dissipation, and Disequilibrium in an Embayment With Complex Bathymetry'. *Journal of Geophysical Research: Oceans*, 123 (11), pp. 7856-7876.

Costa, M. B., Macedo, E. C. & Siegle, E. (2019) 'Wave refraction and reef island stability under rising sea level'. *Global and Planetary Change*, 172 pp. 256-267.

Durai Eswaran, S. R., Sannasiraj, S. A. & Sundar, V. (2020) 'Study on Wave Amplification Using Circular and Elliptical Plates', Trung Viet, N., Xiping, D. and Thanh Tung, T. eds.). *APAC 2019*. Singapore 2020. Springer Singapore, pp. 1123-1126.

Elgar, S., Herbers, T. H. C. & Guza, R. T. (1994) 'Reflection of Ocean Surface Gravity Waves from a Natural Beach'. *Journal of Physical Oceanography*, 24 (7), pp. 1503-1511.

Harris, D. L., Power, H. E., Kinsela, M. A., Webster, J. M. & Vila-Concejo, A. (2018) 'Variability of depth-limited waves in coral reef surf zones'. *Estuarine, Coastal and Shelf Science*, 211 pp. 36-44.

Hutt, J. A., Black, K. P. & Mead, S. T. (2001) 'Classification of Surf Breaks in Relation to Surfing Skill'. *Journal of Coastal Research*, pp. 66-81.

Ito, Y. & Tanimoto, K. (1972) 'Method of Numerical Analysis of Wave Propagation; Application to Wave Diffraction and Refraction ', *Coastal Engineering 1972.* pp. 503-522.

Joevivek, V. J., Chandrasekar, N., Jayangondaperumal, R., Thakur, V. C. & Shree Purniema, K. (2019) 'An interpretation of wave refraction and its influence on foreshore sediment distribution'. *Acta Oceanologica Sinica*, 38 (5), pp. 151-160.

Koutitas, C. & Scarlatos, P. D. (2015) 'Computational modelling in hydraulic and coastal engineering*'.* CRC Press.

Lewis, M., Palmer, T., Hashemi, R., Robins, P., Saulter, A., Brown, J., Lewis, H. & Neill, S. (2019) 'Wave-tide interaction modulates nearshore wave height'. *Ocean Dynamics*, 69

Lynett, P., Liu , P., Sitanggang, K. & Kim, D.-H. (2004) 'Modeling Wave Generation Evolution and Interaction with Depth-Integrated Dispersive Wave Equations COULWAVE Code Manual'*.*

Mandlier, P. G. & Kench, P. S. (2012) 'Analytical modelling of wave refraction and convergence on coral reef platforms: Implications for island formation and stability'. *Geomorphology (Amsterdam, Netherlands)*, 159-160 pp. 84-92.

Masselink, G. (2019) 'Waves', in Finkl, C.W. and Makowski, C. (eds.) *Encyclopedia of Coastal Science.* Cham: Springer International Publishing, pp. 1878-1886.

Mead, S. & Black, K. (2001) 'Field Studies Leading to the Bathymetric Classification of World-Class Surfing Breaks'. *Journal of Coastal Research*, pp. 5-20.

Mendonça, A., Conceição, J., Fortes, C., Capitão, R., Maria, G., Neves, M., Antunes, D., Antunes do Carmo, J. & Moura, T. (2012) 'JWaterwayPortCoastalEngineering'..

Monk, K., Zou, Q. & Conley, D. (2013) 'An approximate solution for the wave energy shadow in the lee of an array of overtopping type wave energy converters'. *Coastal Engineering*, 73 pp. 115–132.

Peak, S. D. (2004) 'Wave refraction over complex nearshore bathymetry'. Thesis. Monterey, California. Naval Postgraduate School.

Rijnsdorp, D. P., Hansen, J. E. & Lowe, R. J. (2020) 'Understanding coastal impacts by nearshore wave farms using a phase-resolving wave model'. *Renewable Energy*, 150 pp. 637-648.

Rogers, W. E. (2020) 'Phase-averaged wave models'*.* World Scientific.

Save the waves coalition (2023) 'World surfing reserves'. [Online]. Available at: https://www.savethewaves.org/wsr/.

Scarfe, B. E., Elwany, M. H. S., Mead, S. T. & Black, K. P. (2003) 'The science of surfing waves and surfing breaks - A review'.

Scarfe, B. E., Healy, T. R. & Rennie, H. G. (2009) 'Research-Based Surfing Literature for Coastal Management and the Science of Surfing: A Review'. *Journal of Coastal Research*, 25 (3), pp. 539-665.

Speranski, N. & Calliari, L. (2001) 'Bathymetric Lenses and Localized Coastal Erosion in Southern Brazil'. *Journal of Coastal Research*, pp. 209-215.

Surfline 'Saunton surf report'. [Online]. Available at: https://www.surfline.com/surf-report/saunton/5842041f4e65fad6a7708e10?camId=5834a06de411dc743a5d52e5.

UK Renewables atlas 'Explore the ABPMER UK renewables atlas'. [Online]. Available at: https://www.renewables-atlas.info/explore-the-atlas/ (Accessed: 10/03/2023).

West, A. (2002) 'Wave-focusing surfing reefs-a new concept'. TU Delft.

Westhuysen, A. J. v. d. (2012) 'Modeling nearshore wave processes'. *ECMWF workshop on Ocean waves*,

Wolf, J. (2008) 'Coastal flooding: Impacts of coupled wave-surge-tide models'. *Natural Hazards*, 49 pp. 241-260.

Yates, E. 'Surfing Saunton Sands'. Honest surf. [Online]. Available at: https://honestsurf.com/surfing-saunton-sands/.

Zhang, Y., Shi, F., Kirby, J. T. & Feng, X. (2022) 'Phase-Resolved Modeling of Wave Interference and Its Effects on Nearshore Circulation in a Large Ebb Shoal-Beach System'. *Journal of Geophysical Research: Oceans*, 127 (10).